



Thermal Conductivity Spectroscopy Technique to Measure Phonon Mean Free Paths

A. J. Minnich,¹ J. A. Johnson,² A. J. Schmidt,³ K. Esfarjani,¹ M. S. Dresselhaus,⁴ K. A. Nelson,² and G. Chen^{1,*}

¹*Department of Mechanical Engineering, Massachusetts Institute of Technology, Cambridge, Massachusetts 02139, USA*

²*Department of Chemistry, Massachusetts Institute of Technology, Cambridge, Massachusetts 02139, USA*

³*Department of Mechanical Engineering, Boston University, Boston, Massachusetts 02215, USA*

⁴*Department of Electrical Engineering and Department of Physics, Massachusetts Institute of Technology, Cambridge, Massachusetts 02139, USA*

(Received 31 May 2011; published 25 August 2011)

Size effects in heat conduction, which occur when phonon mean free paths (MFPs) are comparable to characteristic lengths, are being extensively explored in many nanoscale systems for energy applications. Knowledge of MFPs is essential to understanding size effects, yet MFPs are largely unknown for most materials. Here, we introduce the first experimental technique which can measure MFP distributions over a wide range of length scales and materials. Using this technique, we measure the MFP distribution of silicon for the first time and obtain good agreement with first-principles calculations.

DOI: 10.1103/PhysRevLett.107.095901

PACS numbers: 65.40.-b, 63.20.dd, 63.22.-m

Thermal transport at scales comparable to phonon wavelengths and mean free paths (MFPs) is presently a topic of considerable interest [1–4]. Size effects caused by the macroscopic dimensions of a bulk sample were first considered by Casimir [5]. Recently, nanostructured materials such as nanowires, superlattices, and nanocomposites with strongly reduced thermal conductivities due to phonon scattering at interfaces and boundaries have been reported and are being assessed for use in thermoelectrics applications [3,4,6,7]. Another type of size effect can occur if there is a temperature gradient over length scales comparable to phonon MFPs. In this case, local thermal equilibrium does not exist and the transport is nondiffusive. Transient ballistic transport has been studied using heat-pulse techniques at cryogenic temperatures [8]. A nonlocal theory of heat transport was proposed as a modification of diffusion theory [9]. It was also predicted that the heat conduction from a nanoparticle is significantly reduced from the Fourier law prediction [10].

Despite the crucial importance of the knowledge of phonon MFPs towards understanding and engineering these size effects, MFPs are largely unknown even for bulk materials and few experimental techniques exist to measure them. Traditionally, empirical expressions and simple relaxation time models have been the only means to estimate MFPs [11]. Recent first-principles calculations show that MFPs of phonons relevant to thermal conductivity vary by more than 5 orders of magnitude [12]. Experimentally, inelastic neutron scattering has been used to measure phonon lifetimes in certain materials, but this technique is more suited for single crystal samples [13]. An x-ray diffraction and thermorefectance technique can measure ballistic transport in some structures [14]. Koh *et al.* proposed a technique which uses a variation of modulation frequency to measure MFPs, but this technique is limited by the modulation frequency [15].

Here, we introduce a thermal conductivity spectroscopy technique which can measure MFP distributions over a wide range of length scales and materials. The technique is based on the prediction that the heat flux from a heat source will be lower than that predicted by Fourier's law when some phonon MFPs are longer than the heater dimensions due to nonlocal heat conduction external to the heat source [10]. This prediction was recently confirmed experimentally using a soft x-ray transient grating technique [16]. The authors observed higher thermal resistance between a nickel nanoline and a sapphire substrate than predicted by Fourier's law and attributed this observation to an additional "ballistic resistance." While this experiment measures the total thermal resistance, yielding an average MFP, our technique can distinguish the separate interfacial and substrate resistances, enabling us to extract the thermal conductivity contributions from phonons with different MFPs in the substrate. Considering the frequency dependence of the MFPs is essential because MFPs vary over such a broad length range.

To see how the thermal conductivity spectroscopy technique works, let us examine the transport of phonons from a heated region of diameter D at the surface of a substrate. After a phonon is emitted from the heater, its probability of scattering near the heater depends on the value of the phonon MFPs Λ_ω relative to D , where ω is the phonon frequency. If $D \gg \Lambda_\omega$, the transmitted phonons scatter and relax to a local thermal equilibrium. Alternatively, if $D \ll \Lambda_\omega$, phonons do not scatter near the heater and the transport is ballistic. In this regime, the actual heat flux is lower than the Fourier's law prediction, which assumes the occurrence of nonexistent scattering events [10,16]. This reduction in heat flux is the origin of the ballistic resistance which is observed experimentally [16]. In real materials, the strong frequency dependence of phonon MFPs Λ_ω means that for any value of D comparable to MFPs, the

transport will be quasiballistic: some phonons will be in the diffusive regime, others in the ballistic regime, and intermediate MFP phonons somewhere in between.

The above discussion shows that a measurement of heat transfer in the quasiballistic regime contains information about phonon MFPs. To see why, let us start with the case $D \gg \Lambda_\omega$ and decrease D . For the case of large D , the heat transfer is diffusive and described by Fourier's law. As D decreases, the ballistic thermal resistance will appear when some phonons have $\Lambda_\omega > D$, with the magnitude of the ballistic resistance depending on the importance of a particular group of phonons to the heat transfer. For example, if the ballistic resistance grows significantly as D decreases from 60 to 30 μm , we can conclude that phonons with MFPs $30 \mu\text{m} < \Lambda_\omega < 60 \mu\text{m}$ carry a significant portion of the heat. Our thermal conductivity spectroscopy technique consists of systematically varying D and observing the change in ballistic resistance from one value of D to the next. By doing so, we can infer the contribution of different phonon MFPs to the thermal conductivity based on the change in ballistic resistance. The technique is similar to point contact spectroscopy for electrons in which electron transport becomes ballistic when the contact diameter is comparable to electron MFPs [17].

In principle, the technique can be implemented using a variety of experimental configurations so long as the variable heater size is comparable to the MFPs of the material of interest. Here, we use transient thermoreflectance (TTR) because TTR routinely achieves micron spatial resolution, comparable to phonon MFPs in many materials. In TTR, a pump beam heats a sample, which consists of a substrate of interest coated with a thin metal transducer film. A time delayed probe beam measures the change in reflectance due to the temperature increase induced by the pump beam. Thermal properties are extracted by fitting the resulting temperature decay curve to a thermal model [18].

We demonstrate our thermal conductivity spectroscopy technique by using TTR to measure the thermal properties of a high-purity ($> 20\,000 \Omega\text{m}$) natural Si wafer at cryogenic temperatures. We chose natural silicon because MFPs at low temperatures are hundreds of microns or larger, much bigger than a typical pump beam diameter in the tens of microns range. To perform the experiment, the wafer was coated with 100 nm of Al using electron-beam evaporation. The native oxide of the wafer was removed using an HF etch immediately prior to deposition, giving a high interface conductance $G = 3.5 \times 10^8 \text{ W/m}^2\text{K}$ at $T = 300 \text{ K}$. The thickness of the film was verified using profilometry. Our experimental setup has been described elsewhere [18]. Our thermal model is based on the heat equation in cylindrical coordinates [18], from which we obtain the Al/Si interface conductance G and the Si thermal conductivity k by fitting the experimental data. For diffusive heat transfer, we can accurately measure thermal properties for a variety of materials [18]. However, for

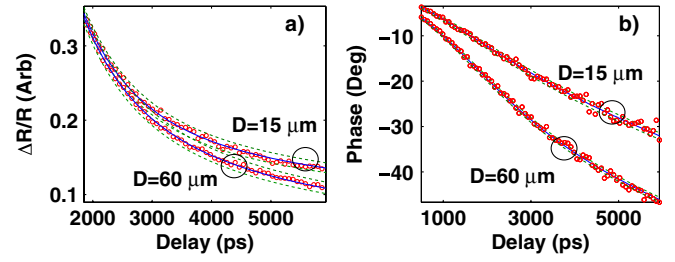


FIG. 1 (color online). Experimental data (symbols) at $T = 90 \text{ K}$ for pump beam diameters $D = 60 \mu\text{m}$ and $D = 15 \mu\text{m}$, along with the (a) amplitude and (b) phase fit to the data from a thermal model (solid lines) and 10% bounds on the fitted thermal conductivity value (dashed lines). The thermal conductivities obtained from the fits are 630 and 480 W/mK , respectively, different from each other and both far from the accepted thermal conductivity of 1000 W/mK [19].

quasiballistic transport the experiment will measure an additional ballistic resistance, the magnitude of which depends on the number of phonon modes with MFPs longer than the pump beam diameter.

Figures 1(a) and 1(b) show representative experimental amplitude and phase signals [$R^2 = X^2 + Y^2$; $\Phi = \tan^{-1}(Y/X)$; where X and Y are the in-phase and out-of-phase signals measured by the lock-in amplifier, respectively], and the fitting curves which are used to extract the thermal conductivity and interface conductance [18]. The data in this figure were taken at $T = 90 \text{ K}$ for pump beam diameters $D = 60 \mu\text{m}$ and $D = 15 \mu\text{m}$. The fits are quite good, but correspond to thermal conductivities of 630 and 480 W/mK , respectively, different from each other and both far from the accepted thermal conductivity of 1000 W/mK at 90 K [19]. A lower measured thermal conductivity indicates that the heat transfer in the substrate is smaller than that predicted by Fourier's law.

Figure 2(a) shows our TTR measurements of the thermal conductivity of Si versus temperature, along with literature values of the thermal conductivity [19] and modeling results which will be explained later in the Letter. The

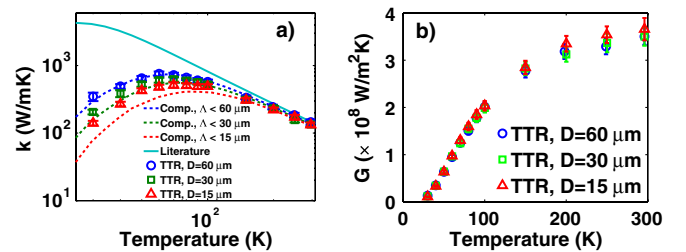


FIG. 2 (color online). (a) Experimentally measured thermal conductivity k (symbols), computed thermal conductivity which only includes the contributions of the indicated MFP or smaller (dashed lines), and the literature thermal conductivity (solid line, Ref. [19]) of natural silicon. (b) Measured interface conductance G of the Al/Si interface. The interface conductance does not depend on beam diameter.

symbols and error bars represent the average and standard deviation, respectively, of measurements taken on several samples at four modulation frequencies from 3–12 MHz. Three different pump diameters (defined as the width of the beam where the intensity has dropped to $1/e^2$ of the peak value) of 60, 30, and 15 μm were used with a constant probe beam diameter of 11 μm . The ellipticities ϵ of the pump and probe beams were $0.8 < \epsilon < 1$. The pump beam power was adjusted so that the intensity remained the same for each diameter; the probe power remained constant. Care was taken to ensure that the steady-state and transient temperature rise of the sample did not exceed 2 K. The lateral spreading of heat in the Al film is estimated to be less than 1 μm in the temperature range of the experiment. All measurements were taken under high vacuum (1×10^{-5} torr). The temperature of the sample was monitored using a silicon diode placed next to the sample. At room temperature, where MFPs are shorter, our measurements are independent of diameter and in good agreement with literature values, but our measurements begin to diverge from the literature values below around 200 K and a diameter dependence of the thermal conductivity appears. This discrepancy is because the ballistic thermal resistance measured by the experiment increases as temperature decreases due to the rapid increase in MFPs as described in the introduction. A smaller thermal conductivity is measured for smaller pump beam diameters because the ballistic resistance is larger around a smaller heated region.

The thermal interface conductance values between Al and Si measured using different laser beam diameters are shown in Fig. 2(b), and no diameter dependence is observed, indicating that ballistic transport in the silicon substrate is responsible for the observed results. In the transient grating experiments in Ref. [16], the total thermal resistance from the interface and substrate was measured, making it difficult to study transport specifically in the substrate.

Koh *et al.* observed a laser modulation frequency dependence of the measured thermal conductivity of semiconductor alloys in a pump-probe experiment and interpreted the result by assuming that some phonons are ballistic over the cross-plane thermal diffusion length [15]. Our measured thermal conductivity was independent of the modulation frequency, indicating that the pump diameter is the dominant length scale rather than the one-dimensional thermal penetration depth.

To further understand our measurements, we need to examine how ballistic modes affect the heat flux. In principle the transport in the quasiballistic regime can be calculated using the Boltzmann transport equation (BTE). However, solving the BTE in multiple dimensions is difficult and computationally expensive, and requires the unknown MFPs to be specified. Therefore, rather than solving the BTE, we make the following approximation. We divide the phonons in the substrate into a diffusive group and

a ballistic group. The diffusive group has short MFPs $\Lambda_\omega < D$ so that a local thermal equilibrium exists among these modes. The ballistic group has MFPs $\Lambda_\omega > D$ which are assumed to be effectively infinite. If we examine the BTE [10], we find that this assumption completely decouples the ballistic group from the rest of the phonons. As shown earlier, while these ballistic modes still carry heat, they carry significantly less heat than predicted by Fourier's law. Our approximation is that the ballistic group does not contribute to thermal transport due to the effectively infinite ballistic resistance; the thermal conductivity measured in the experiment is only due to the diffusive group [15].

To verify this model we can calculate the expected thermal conductivity if the ballistic group does not contribute to the measured thermal conductivity. We compute the phonon MFPs in Si from first principles, following a similar procedure as described in Ref. [12]. Briefly, density functional theory is employed to compute the potential energy derivative in Si crystals. Perturbation to the atomic positions is used to extract the third and fourth order anharmonic coefficients of the potentials and Fermi's golden rule is used to compute relaxation times, while other quantities such as the dispersion and group velocity are computed from the harmonic force constants [20,21]. Using the computed information, the thermal conductivity can be determined from $k = \sum_q C_q v_{x,q}^2 \tau_q$, where q is the phonon wave vector and C_q , $v_{x,q}$, and τ_q are the specific heat, group velocity, and relaxation time of a phonon with wave vector q , respectively. The ballistic group can be excluded by removing terms from the sum according to the MFP of the mode. The results of the calculation are shown as the dashed lines in Fig. 2(a). The agreement between our measurements and this simple cutoff model is reasonably good. Obtaining quantitative agreement is difficult because the thermal conductivity value is very sensitive to the isotope concentration, which is not precisely known. We use a typical value fitted from thermal conductivity measurements of natural silicon [19].

We can now use our measurements to determine the thermal conductivity accumulation of silicon as a function of MFP [22]. In our experiment, we have measured the thermal conductivity of the diffusive group of phonons with MFPs shorter than the pump beam diameter. Thus, normalizing the measured thermal conductivities by the true thermal conductivity will give the fraction of the thermal conductivity contributed by phonons with $\Lambda_\omega < D$, which is simply the thermal conductivity accumulation distribution. Our experimental measurements of this distribution, along with that predicted by the first-principles calculations, are shown in Fig. 3. The agreement between the experiment and the calculation is again reasonably good. Note that no assumption about the MFPs was used in the analysis of the experimental data: the data were analyzed using the heat equation to determine the apparent thermal conductivity, and this value was

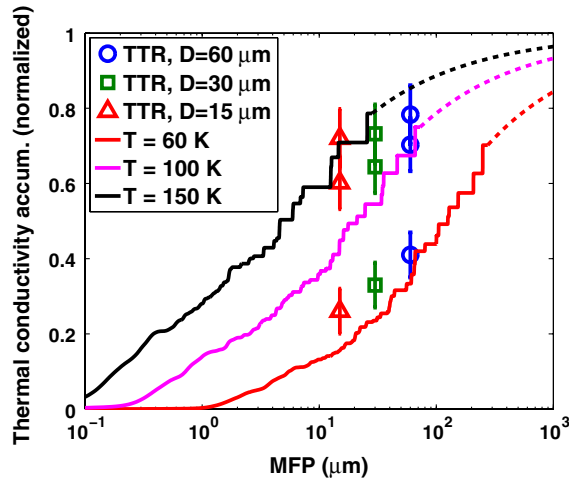


FIG. 3 (color online). Thermal conductivity accumulation distribution experimental measurements (symbols) and first-principles calculations (lines) of natural silicon versus MFP. The symbols and error bars represent the average and standard deviation, respectively, of measurements taken on several samples at different locations and modulation frequencies. The dashed line is an extrapolation of the first-principles calculations to long wavelengths; the extrapolation is required because of the finite number of reciprocal space points used in the calculation.

compared to the results of the first-principles calculations. The consistency between these two approaches is encouraging, and indicates that our technique is accurately measuring the thermal conductivity contributions from different phonon MFPs.

In summary, we have demonstrated the first experimental technique which can measure the MFPs of phonons relevant to thermal conduction across a wide range of length scales and materials. While empirical expressions and simple relaxation time models have traditionally been the only means to estimate MFPs, our technique enables a direct measurement of how heat is distributed among phonon modes. Although our demonstration of the thermal conductivity spectroscopy technique is for length scales in the tens of microns range, the technique can be extended to an arbitrary length range and to arbitrary materials by changing the heater dimension using related optical techniques or lithographically patterned heaters. Our successful application of the technique at submicron length scales in sapphire, GaAs, and Si membranes will be described in subsequent publications. Considering the crucial importance of the knowledge of MFPs to understanding and engineering size effects, we expect the technique to be useful for a variety of energy applications, particularly for thermoelectrics.

This material is partially based upon work supported as part of the “Solid State Solar-Thermal Energy Conversion

Center (S3TEC),” an Energy Frontier Research Center funded by the U.S. Department of Energy, Office of Science, Office of Basic Energy Sciences under Grant No. DE-SC0001299/DE-FG02-09ER46577 (G. C., J. J., K. E., K. N., and M. S. D.), by the Center for Clean Water and Clean Energy at MIT and KFUPM (A. M.), and by the NSF (A. M.). The authors would like to thank Alexei A. Maznev for useful discussions.

*gchen2@mit.edu

- [1] D. G. Cahill, W. K. Ford, K. E. Goodson, G. D. Mahan, A. Majumdar, H. J. Maris, R. Merlin, and S. R. Phillpot, *J. Appl. Phys.* **93**, 793 (2003).
- [2] J.-K. Yu, S. Mitrovic, D. Tham, J. Varghese, and J. R. Heath, *Nature Nanotech.* **5**, 718 (2010).
- [3] A. I. Hochbaum, R. Chen, R. D. Delgado, W. Liang, E. C. Garnett, M. Najarian, A. Majumdar, and P. Yang, *Nature (London)* **451**, 163 (2008).
- [4] G. Pernot *et al.*, *Nature Mater.* **9**, 491 (2010).
- [5] H. Casimir, *Physica (Amsterdam)* **5**, 495 (1938).
- [6] A. I. Boukai, Y. Bunimovich, J. Tahir-Kheli, J.-K. Yu, W. A. Goddard III, and J. R. Heath, *Nature (London)* **451**, 168 (2008).
- [7] B. Poudel *et al.*, *Science* **320**, 634 (2008).
- [8] R. J. von Gutfeld and A. H. Nethercot, *Phys. Rev. Lett.* **12**, 641 (1964).
- [9] G. D. Mahan and F. Claro, *Phys. Rev. B* **38**, 1963 (1988).
- [10] G. Chen, *J. Heat Transfer* **118**, 539 (1996).
- [11] M. G. Holland, *Phys. Rev.* **132**, 2461 (1963).
- [12] A. Ward and D. A. Broido, *Phys. Rev. B* **81**, 085205 (2010).
- [13] A. D. Christianson *et al.*, *Phys. Rev. Lett.* **101**, 157004 (2008).
- [14] M. Highland, B. C. Gundrum, Y. K. Koh, R. S. Averback, D. G. Cahill, V. C. Elarde, J. J. Coleman, D. A. Walko, and E. C. Landahl, *Phys. Rev. B* **76**, 075337 (2007).
- [15] Y. K. Koh and D. G. Cahill, *Phys. Rev. B* **76**, 075207 (2007).
- [16] M. E. Siemens, Q. Li, R. Yang, K. A. Nelson, E. H. Anderson, M. M. Murnane, and H. C. Kapteyn, *Nature Mater.* **9**, 26 (2009).
- [17] G. Deutscher, *Nature (London)* **397**, 410 (1999).
- [18] A. J. Schmidt, X. Chen, and G. Chen, *Rev. Sci. Instrum.* **79**, 114902 (2008).
- [19] A. V. Inyushkin, A. N. Taldenkov, A. M. Gibin, A. V. Gusev, and H. J. Pohl, *Phys. Status Solidi (c)* **1**, 2995 (2004).
- [20] K. Esfarjani and H. T. Stokes, *Phys. Rev. B* **77**, 144112 (2008).
- [21] K. Esfarjani, G. Chen, and H. T. Stokes, *Phys. Rev. B* **84**, 085204 (2011).
- [22] C. Dames and G. Chen, in *CRC Thermoelectrics Handbook: Macro to Nano*, edited by D. Rowe (CRC Press, Boca Raton, FL, 2005).